

Dynamic properties of human brain structure: learning-related changes in cortical areas and associated fibre connections

Marco Taubert, Bogdan Draganski, Alfred Anwander, Karsten Müller, Annette
Horstmann, Arno Villringer & Patrick Ragert

Supplemental material

RESULTS

Behavioural results

Improvements in motor performance were consolidated between subsequent TD's (no significant difference between the last and the first trial between consecutive TD's; $p > 0.05$). To test the long-term stability of the acquired motor skill, we conducted a retention test (15 trials) three months after the end of the learning period (Ryan, 1965; Schmidt and Lee, 1999). We compared mean and end-performance on TD 6 with initial performance in the retention test. The results showed retention of mean performance (TD 6) of about $88 \pm 1.4\%$ (mean \pm s.e.m.) and no significant differences between end-performance levels on TD 6 and the first retention trials ($p > 0.05$; see Fig. 1C and Fig. S1).

Initial grey matter volume predicts motor performance on TD 6

In order to test whether baseline GM values predict performance, we used a correlation analysis with average performance on TD6 for each subject as dependant variable. After correcting for total grey matter volume, age and gender, we found that grey matter in the right temporal pole ($x = 33, y = 22, z$

= -32; Z = 4.99) and the right superior temporal gyrus (x = 49, y = -6, z = -7; Z = 4.7) correlated positively with performance on TD6 ($p < 0.05$ corrected; see Fig. S6), suggesting that long-term memory representations might have a significant impact on future motor performance improvements (Fink et al., 1996).

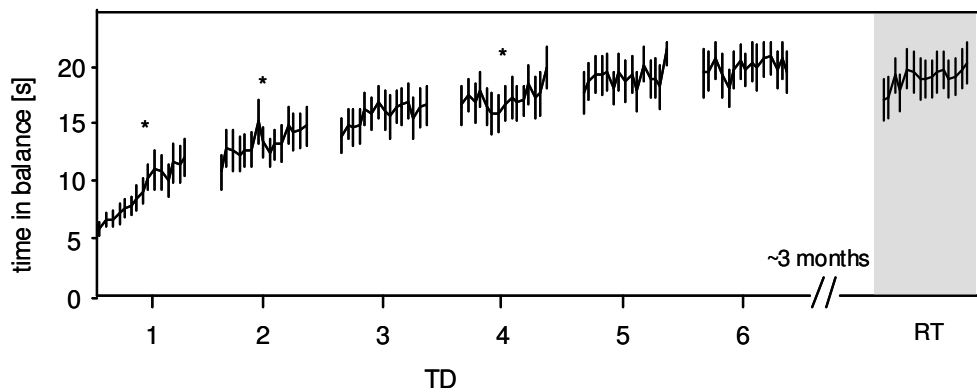


Figure S1. Within-session improvements during the time course of learning and retention test performance. Asterisks indicate within-session improvements on TD 1, TD 2 as well as on TD 4 (repeated measures ANOVA; main effect of TRIAL; TD 1: $F(14, 195) = 7.2$; $p < 0.001$; TD 2: $F(14, 195) = 2.8$; $p < 0.022$; TD 4: $F(14, 195) = 2.7$; $p < 0.021$). Major thick lines indicate mean performance for each trial across subjects; error bars indicate standard error of mean (s.e.m.).

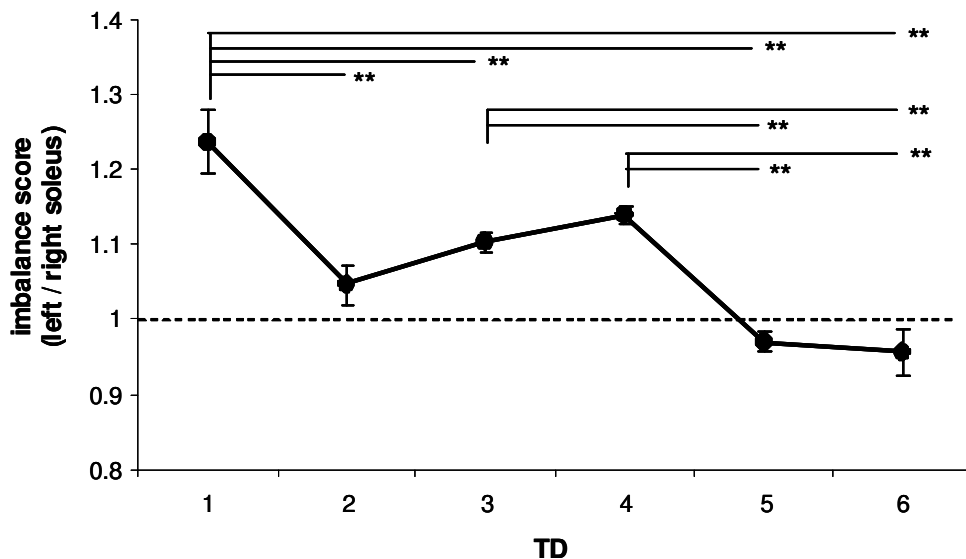


Figure S2. Between-session adaptations in muscular imbalances during the time course of learning (repeated measures ANOVA with factor TD (1-6): $F(14, 70) = 17.1$; $p < 0.001$). Deviations from 1 (y -axis; dotted line) indicate imbalances between left and right soleus EMG activity during task execution. Asterisks indicate between-session changes (** $p < 0.01$). Error bars indicate standard error of mean (s.e.m.).

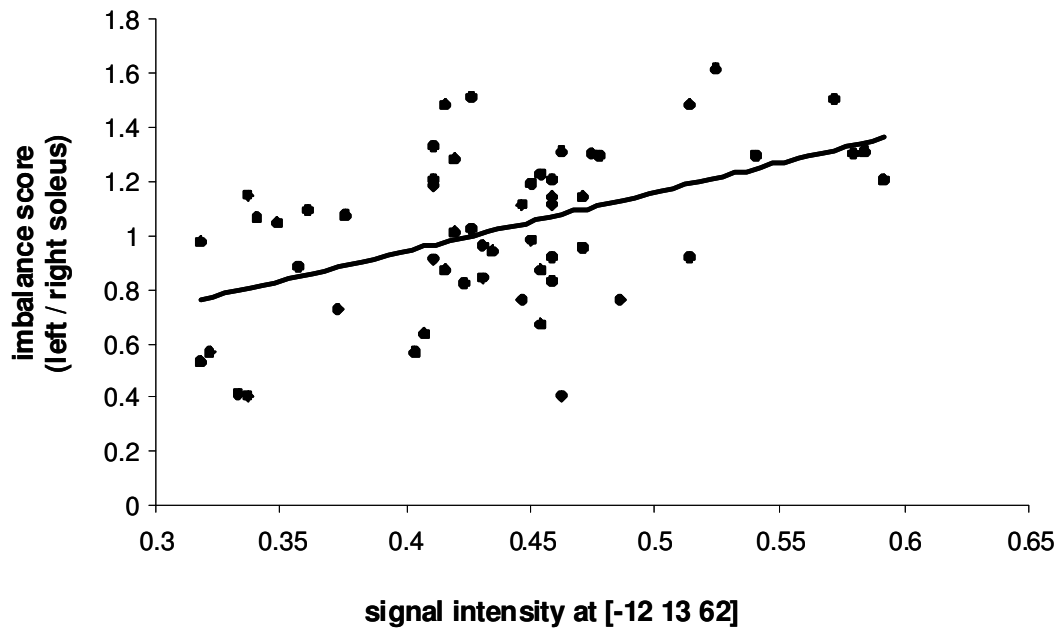


Figure S3. Positive correlation between individual adaptations in muscular imbalances and signal intensity at [-12 13 62] (peak voxel from parametric correlation analysis in left SMA) across all four scanning time points ($r = 0.498$; $p < 0.001$).

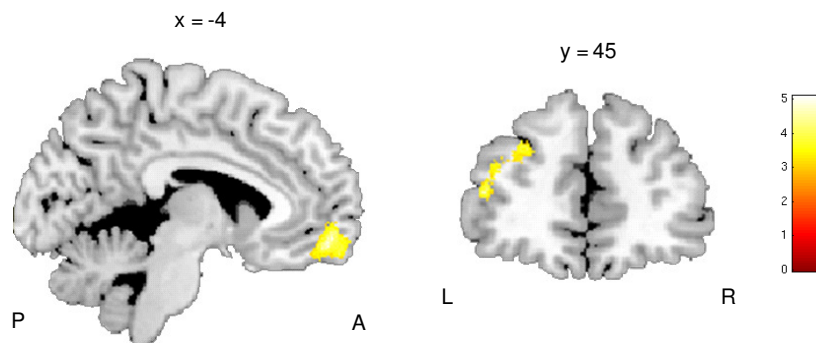


Figure S4. GM increases from baseline to the end of the learning period (paired t-test, $s_1 < s_4$). Sagittal section shows GM changes in left medial OFC

and coronal section in left IFG/MFG. Images are shown at $p < 0.05$ corrected on cluster-level and $p < 0.005$ uncorrected on voxel-level. Bar indicates t-value.

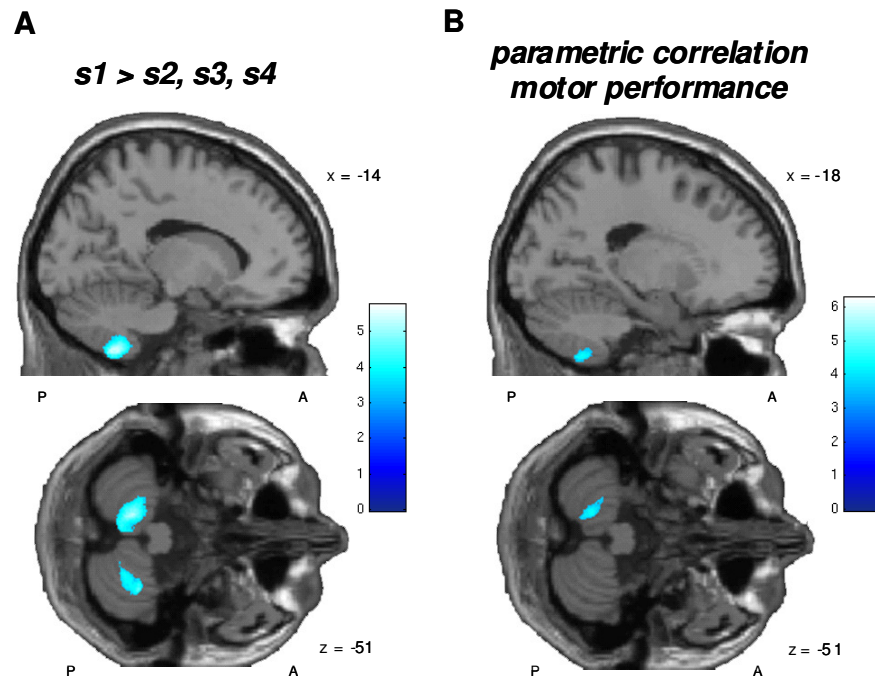


Figure S5. GM reduction across the whole learning period in bilateral cerebellum (lobule VIII). (A) GM reduction in the learning period (s2, s3 and s4) as compared to baseline (s1). (B) Negative linear correlation between improvements in motor performance and GM volume. See Table S5 for all regions showing GM reductions during learning. All images are shown at $p < 0.05$ (corrected). Bars indicate t-values.

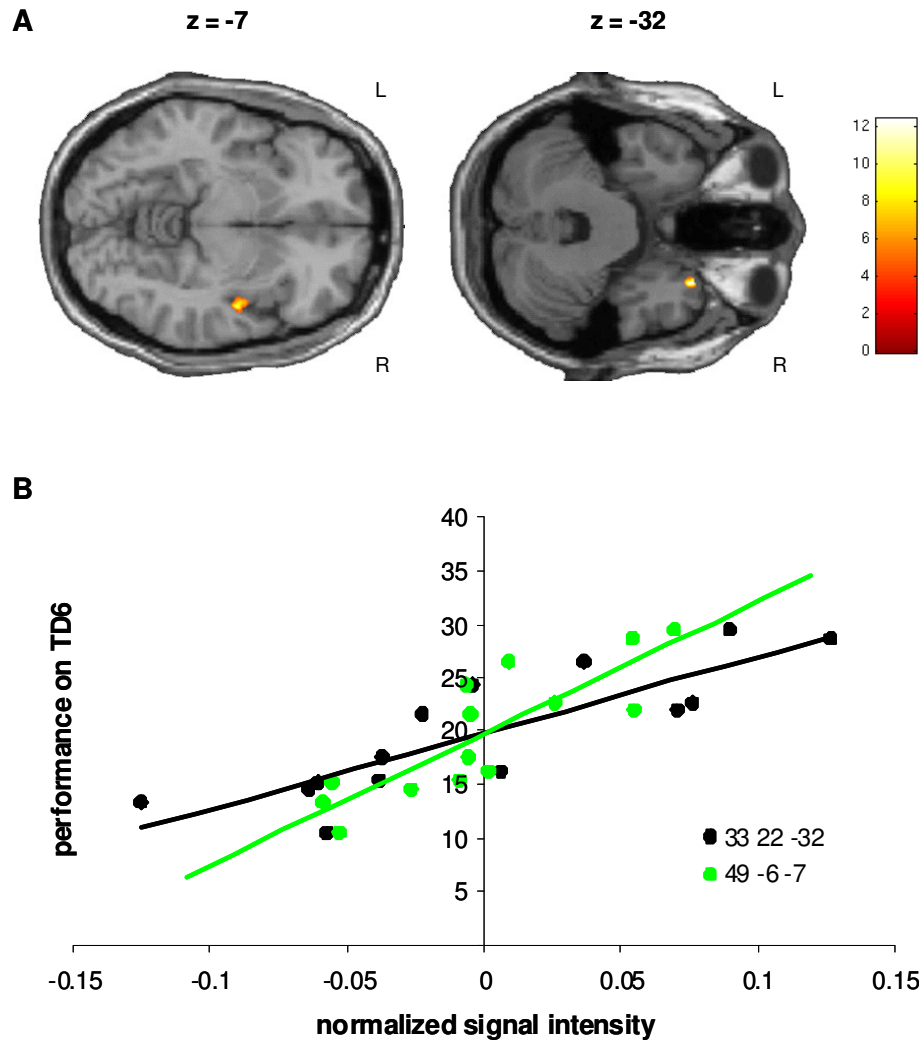


Figure S6. Baseline GM volume in right temporal pole and right superior temporal gyrus predict end-performance level (TD6) in the whole-body balancing task. (A) Axial slices indicate significant clusters ($p < 0.05$ corrected). (B) Scatter plot show positive correlation between performance on TD6 and peak voxel signal intensities in temporal pole (black) and superior temporal gyrus (green) at baseline (s1). Bar indicates t-value.

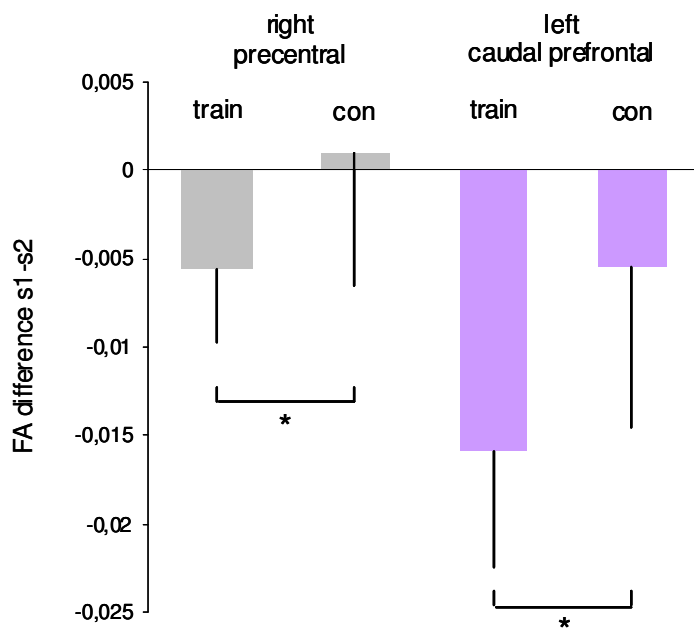
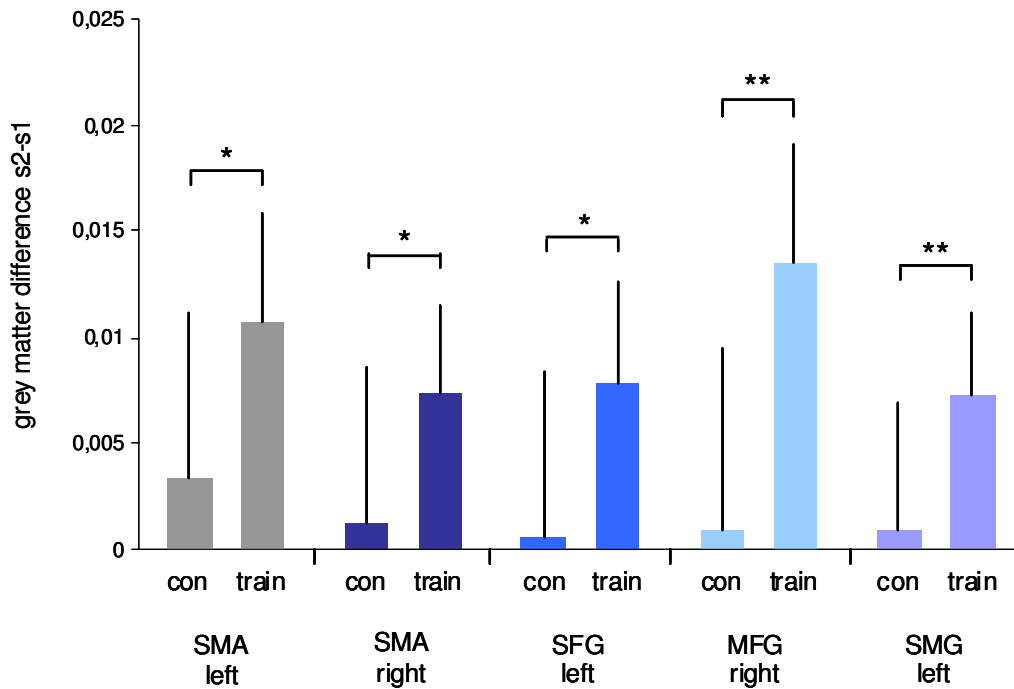


Figure S8. Interaction effects between training (train) and control (con) group for FA changes from s1 to s2 (* $p < 0.05$). Error bars indicate SD.

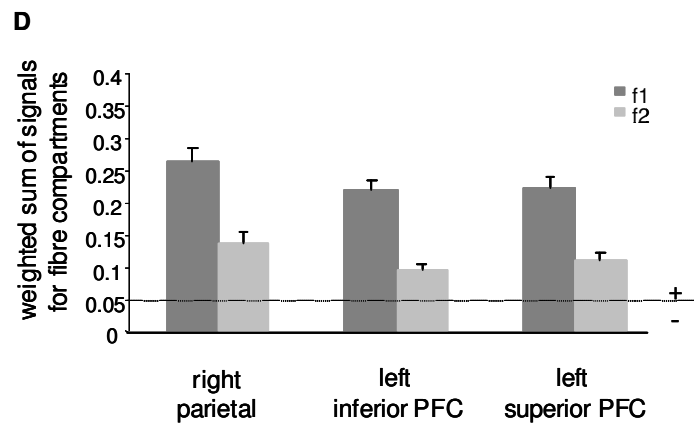
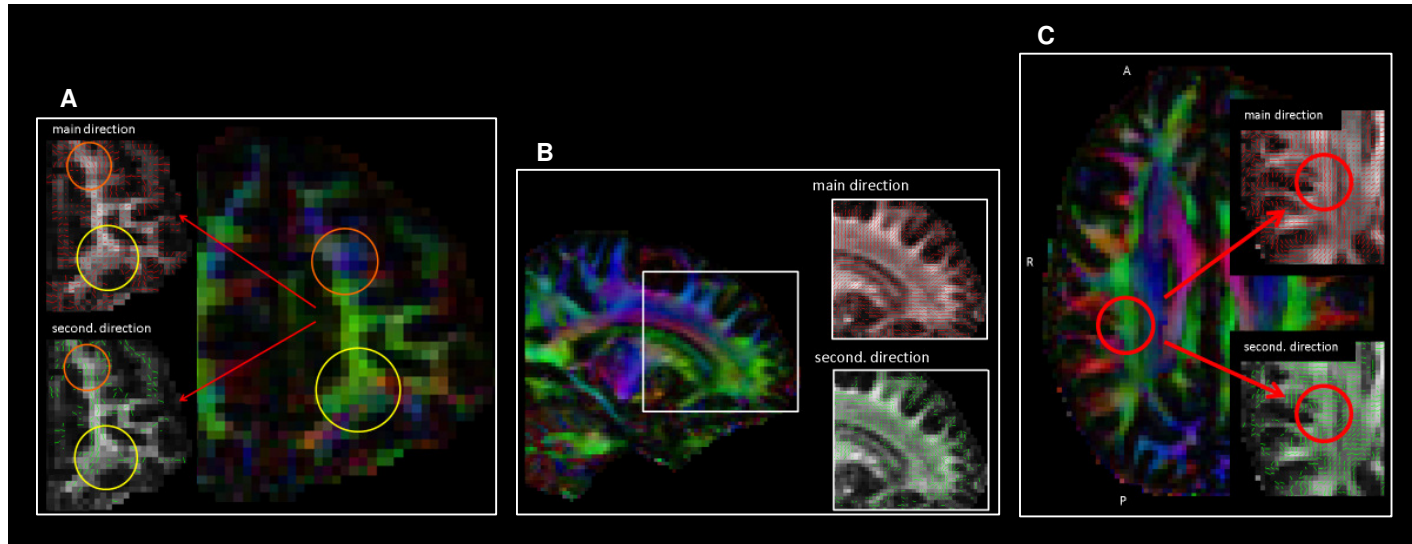


Figure S9. Crossing fibres in clusters showing decreases in FA in correlation with performance improvements during learning in one representative subject. (A) Left: Coronal sections show main (red) and secondary (light green) diffusion directions in left ventral (yellow square) and dorsal (orange square) prefrontal clusters superimposed on the individual FA image. Right: Individual color-coded FA image for diffusion tensor orientation in coronal section (green: anterior – posterior; blue: inferior – superior; red: medial – lateral). (B) Left: Sagittal section of color-coded FA image for diffusion tensor orientation. Right: Main (red) and secondary (light green) diffusion directions in the prefrontal lobe in sagittal plane. The major fibre direction in the prefrontal clusters (in A and B) can be attributed to anterior - posterior oriented thalamo-cortical and transcallosal fibres (Mori, 2005). In contrast, the secondary fibre bundles likely correspond to prefrontal association fibres connecting distinct prefrontal regions (Jacobson and Trojanowski, 1977; Pucak et al., 1996; Woo et al., 1997). (C) Left: Individual color-coded FA image for diffusion tensor orientation in axial section. Red square indicates location of right parietal white matter region. Right: Main (red) and secondary (light green) diffusion directions in right parietal white matter region. All images for main and secondary diffusion direction were thresholded at an f-value of 0.05. (D) Bars indicate average weighted sum of signals (partial volume fraction) for major (f1; dark grey bar) and secondary (f2; light grey bar) fibre bundles in all voxel in right parietal, left ventral and left dorsal prefrontal white matter clusters derived from baseline scan s1 from all subjects. Error bars indicate s.e.m. Dashed horizontal line represents threshold at an f-value of 0.05.

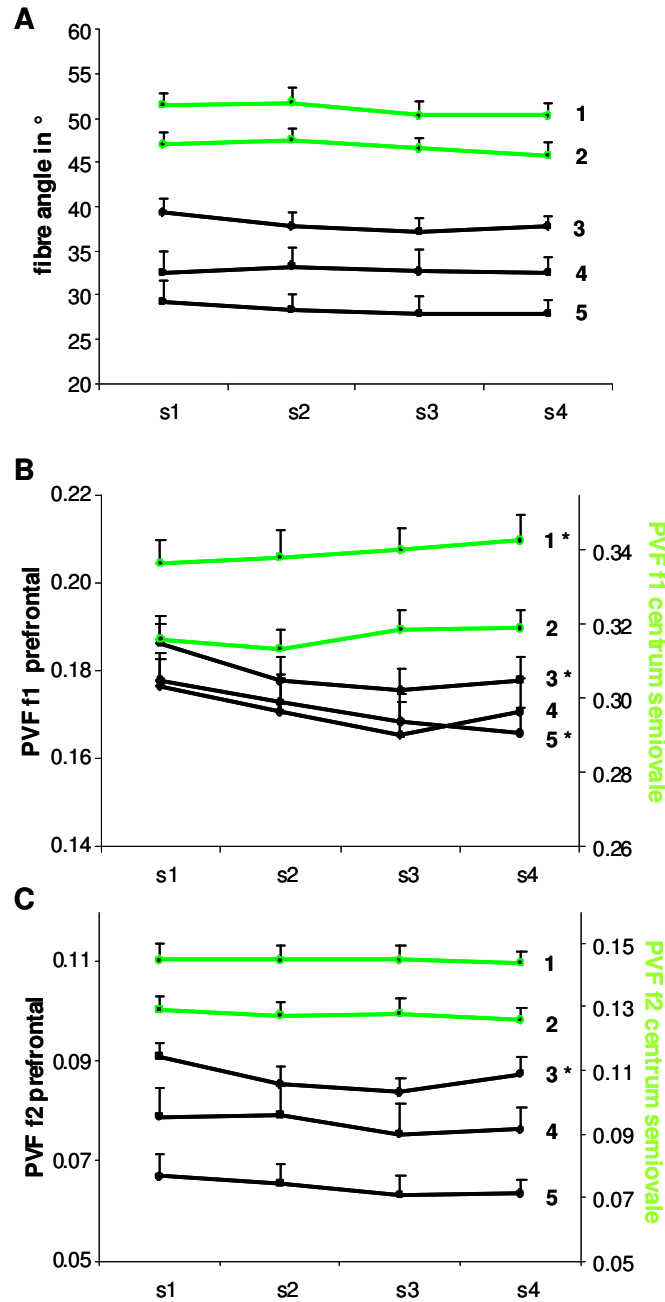


Figure S10. Learning-induced changes in (A) intermediate fibre angle between major and secondary fibre bundle, partial volume fraction (PVF) for major (B; f1) and secondary (C; f2) diffusion direction in five region of interests (from parametric correlation analyses) after scalar re-assignment (Jbabdi et al., 2010). Light green lines (right y-axis in B and C; 1 and 2) represent changes in ROI in bilateral anterior centrum semiovale (see Table S3) sharing a close spatial relationship to initial GM changes in SMA (see Fig. 3A). Black lines (left y-axis in B and C) represent changes in ROI in bilateral dorsal prefrontal (3 and 4) and left ventral prefrontal WM (5; see Table S2) sharing a close spatial relationship to GM changes in left SFG, right MFG and left sOFC (see Tab. S1). Asterisks indicate significant main effect of TIME (s1, s2, s3, s4) with $p < 0.05$.

grey matter expansion*	hemisphere	coordinates (x, y, z)	Z value	cluster size	p value**
<u>s1 < s2, s3, s4</u> supplementary motor areas	L	-12, 13, 64	4,35	1684	<0.001
superior frontal gyrus	L	-22, 53, 20	4,16	724	0.049
middle frontal gyrus	R	41, 29, 32	3,85	2539	0.003***
medial orbitofrontal cortex	L	-7, 53, -12	4,22	842	0.027
<u>s1 < s2</u> supplementary motor areas	L	-8, -2, 69	4,74	5301	<0.001
supplementary motor areas	R	11, 22, 59	4,74	4331	<0.001
superior frontal gyrus	L	-22, 49, 20	4,35	1006	0.005
middle frontal gyrus	R	28, 45, 28	4,73	6270	<0.001
supramarginal gyrus	L	-57, -27, 30	5,00	2888	<0.001
<u>s1 < s4</u> medial orbitofrontal cortex	L	-6, 57, -9	3,68	1578	<0.001***
inferior frontal gyrus	L	-43, 46, 12	3,71	1119	<0.001***
<u>positive correlation with muscular imbalances</u> supplementary motor areas	L	-12, 13, 62	4,74	1140	<0.001
<u>positive correlation with motor performance</u> superior orbitofrontal cortex	L	-29, 61, -7	4,48	550	0.026

*anatomical regions as defined by the labelling library WFU-Pick Atlas/aal-Atlas

**cluster-level *p* values after $p < 0.001$ (uncorrected) and non-stationary cluster-extent correction with $p < 0.05$

***trends obtained with liberal uncorrected threshold of $p < 0.005$ and non-stationary cluster-extent correction with $p < 0.05$

Table S1. Statistical significance for grey matter expansion during motor skill learning.

White matter FA	hemisphere	coordinates (x, y, z)	Z value	cluster size	p value**
<i>s1 > s2, s3, s4</i>					
dorsal prefrontal	L	-16, 58, 26	4,16	109	0.036
dorsal prefrontal	R	16, 56, 30	4,58	118	0.029
<i>s1 > s2</i>					
dorsal prefrontal	L	-40, 30, 38	4,65	155	0.009
precentral	R	48, -18, 48	4,04	139	0.012
<i>negative correlation with muscular imbalances</i>					
superior parietal	L	-32, -64, 50	4,77	132	0.005
occipital white	R	20, -94, 6	4,61	225	<0.001
cingulum	L	-8, -14, 44	3,74	113	0.008
<i>negative correlation with motor performance</i>					
inferior prefrontal	L	-20, 50, -8	4,29	54	0.026
dorsal prefrontal	L	-14, 42, 22	4,06	57	0.02
inferior parietal	R	38, -40, 28	4,83	85	0.004

**cluster-level p values after p<0.001 (uncorrected) and non-stationary cluster-extent correction with p<0.05

Table S2. Statistical significance for FA changes during motor skill learning.

White matter MD	hemisphere	coordinates (x, y, z)	Z value	cluster size	p value**
<u>s1 < s2, s3, s4</u> inferior parietal	R	46, -34, 28	3,63	55	0.032
cerebellum	R	24, -74, -34	3,59	65	0.016
<u>s1 < s2</u> inferior parietal	R	50, -36, 26	4,36	137	0.005
postcentral	R	38, -36, 64	4,29	56	0.014
<u>positive correlation with muscular imbalances</u> cerebellum	L	-20, -50, -44	4,23	100	0.002
cerebellum	R	20, -72, -32	4,21	47	0.033
<u>negative correlation with muscular imbalances</u> superior parietal	L	-34, -62, 52	5,51	263	<0.001
<u>negative correlation with motor performance</u> brainstem	L	-6, -20, -14	5,43	83	0.003
anterior centrum semiovale	L	-20, 6, 36	5,35	189	<0.001
anterior centrum semiovale	R	22, 6, 46	5,16	255	<0.001
internal capsule	R	26, -14, 18	4,98	130	<0.001
<u>positive correlation with motor performance</u> inferior parietal	R	58, -36, 14	5,12	633	<0.001
superior temporal	R	52, -8, -2	4,81	219	<0.001

**cluster-level *p* values after $p < 0.001$ (uncorrected) and non-stationary cluster-extent correction with $p < 0.05$

Table S3. Statistical significance for MD changes during motor skill learning.

<i>ventral prefrontal $\lambda_{ }$ and λ_{\perp}</i>	<i>hemisphere</i>	<i>coordinates (x, y, z)</i>	<i>Z value</i>	<i>cluster size</i>	<i>p value**</i>
<i>negative correlation with motor performance</i>					
$\lambda_{ }$	L	-24, 60, -6	4,40	249	0.014
λ_{\perp}	L	-22, 57, -2	4,20	75	0.031

**cluster-level *p* values after $p < 0.001$ (uncorrected) and non-stationary cluster-extent correction with $p < 0.05$

Table S4. Statistical significance for $\lambda_{||}$ and λ_{\perp} changes in ventral prefrontal white matter during motor skill learning.

grey matter reduction*	hemisphere	coordinates (x, y, z)	Z value	cluster size	p value**
<u><i>s1 > s2, s3, s4</i></u>					
putamen/orbitofrontal (inferior) cortex	R	30, 29, -18	5,00	3452	<0.001
cerebellar lobule VIII	L	-17, -54, -55	4,95	1954	<0.001
cerebellar lobule VIII	R	34, -48, -50	4,20	1170	0.003
middle temporal gyrus	R	62, -45, -7	4,01	2044	<0.001
inferior occipital gyrus	L	-37, -75, -13	4,42	1005	0.005
<u><i>s1 < s4</i></u>					
putamen/insular cortex	L	-29, 14, 7	4,75	3843	<0.001
putamen	R	22, 13, -3	4,15	3438	<0.001
cerebellar lobule VIII	L	-24, -48, -46	4,32	4852	<0.001
cerebellar lobule VIII	R	21, -60, -44	4,29	2257	<0.001
middle temporal gyrus	R	52, -53, -9	5,67	14062	<0.001
inferior occipital gyrus	L	-31, -90, -13	4,83	4559	<0.001
<u><i>negative correlation with motor performance</i></u>					
inferior orbitofrontal cortex	R	27, 26, -17	4,79	5255	<0.001
cerebellar lobule VIII	L	-26, -41, -45	4,43	1554	<0.001
supramarginal gyrus	R	63, -28, 35	4,91	1732	<0.001
middle temporal gyrus	R	58, -60, 5	4,14	2931	<0.001
inferior occipital gyrus	L	-40, -87, -2	4,38	2055	<0.001

*anatomical regions as defined by the labelling library WFU-Pick Atlas/aal-Atlas

**cluster-level p values after $p < 0.001$ (uncorrected) and non-stationary cluster-extent correction with $p < 0.05$

Table S5. Statistical significance for grey matter reductions during motor skill learning.

DISCUSSION

Early and late grey matter changes in lateral prefrontal cortex

The lateral prefrontal cortex (including SFG and MFG) is associated with attentional processing during motor learning (Passingham, 1993). We suggest that GM changes might reflect the importance of focussed attention to keep up with board perturbations to maintain and further improve postural control. The lateral prefrontal cortex has been previously shown to be involved in balance control based on whole-body perturbations (Mihara et al., 2008). Importantly, in our study, subjects reached an average time in balance of 20 seconds on the last training day (TD 6), which is 66% of the possible performance maximum in this task (30 s). Thus, attentional load could be demanding even in the late learning period because there was still space for further performance improvements. Additionally, task performance involved postural control on an unstable platform, which requires a high attentional load during task performance even in later learning phases.

Grey matter reduction

We observed significant grey matter reduction across the whole learning period in motor (bilateral cerebellum), limbic (bilateral ventral putamen and right inferior orbitofrontal cortex) and visual (right middle temporal gyrus and left inferior occipital gyrus) circuits. Grey matter reductions were unexpected because no previous study reported learning-induced grey matter reductions (Draganski et al., 2004; Boyke et al., 2008; Ilg et al., 2008). Thus, we can only speculate about their functional role for human motor skill learning.

Compared to grey matter expansion, the initial phase of learning (s1 - s2) was not significantly affected by grey matter reductions. Reductions emerged in the later phases of learning (s1 - s4 and parametric correlation with motor performance). On the one hand, this could be referred to homeostatic regulation of total brain volume to normalize intracranial pressure due to initial grey matter expansion (Draganski and May, 2008). However, if these were true, one would expect grey matter reduction in task-independent regions in close proximity to grey matter expansion. We observed grey matter reductions in functional e. g. motor-related cerebellar regions implicated in vestibular control (Ito, 1986). Alternatively, synaptic pruning (Huttenlocher, 1979), decreased synapse head-size due to long-term depression (Ito, 1986; Zhou et al., 2004) or proliferation of intracortical axons (Strata and Rossi, 1998) could be discussed as possible mechanisms underlying grey matter reduction. Furthermore, compared to cortical regions where we observed learning-related grey matter expansion (e.g. left OFC), we were not able to identify FA or MD alterations in adjacent white matter regions pointing to fundamentally distinct neural mechanisms of grey matter expansion and reduction. However, the functional impact and underlying mechanism of learning-induced grey matter reductions is not known and needs to be addressed in future studies.

References:

- Boyke J, Driemeyer J, Gaser C, Buchel C, May A (2008) Training-induced brain structure changes in the elderly. *J Neurosci* 28:7031-7035.
- Draganski B, May A (2008) Training-induced structural changes in the adult human brain. *Behav Brain Res* 192:137-142.
- Draganski B, Gaser C, Busch V, Schuierer G, Bogdahn U, May A (2004) Neuroplasticity: changes in grey matter induced by training. *Nature* 427:311-312.
- Fink GR, Markowitsch HJ, Reinkemeier M, Bruckbauer T, Kessler J, Heiss WD (1996) Cerebral representation of one's own past: neural networks involved in autobiographical memory. *J Neurosci* 16:4275-4282.
- Huttenlocher PR (1979) Synaptic density in human frontal cortex - developmental changes and effects of aging. *Brain Res* 163:195-205.
- Ilg R, Wohlschläger AM, Gaser C, Liebau Y, Dauner R, Woller A, Zimmer C, Zihl J, Muhlau M (2008) Gray matter increase induced by practice correlates with task-specific activation: a combined functional and morphometric magnetic resonance imaging study. *J Neurosci* 28:4210-4215.
- Ito M (1986) Long-term depression as a memory process in the cerebellum. *Neurosci Res* 3:531-539.
- Jacobson S, Trojanowski JQ (1977) Prefrontal granular cortex of the rhesus monkey. I. Intrahemispheric cortical afferents. *Brain Res* 132:209-233.
- Jbabdi S, Behrens TE, Smith SM (2010) Crossing fibres in tract-based spatial statistics. *Neuroimage* 49:249-256.
- Mihara M, Miyai I, Hatakenaka M, Kubota K, Sakoda S (2008) Role of the prefrontal cortex in human balance control. *Neuroimage* 43:329-336.
- Mori S, Wakana, S., Nagae-Poetscher, L.M., Zijl, P.C.M. (2005) *MRI Atlas of Human White Matter*. Amsterdam: Elsevier.
- Passingham R (1993) *The Frontal Lobes and Voluntary Action*. Oxford: Oxford University Press.
- Pucak ML, Levitt JB, Lund JS, Lewis DA (1996) Patterns of intrinsic and associational circuitry in monkey prefrontal cortex. *J Comp Neurol* 376:614-630.
- Ryan ED (1965) Retention of Stabilometer Performance Over Extended Periods of Time. *Research Quarterly*:46-51.
- Schmidt RA, Lee TD (1999) *Motor Control and Learning: A Behavioral Emphasis*. Champaign: Human Kinetics.
- Strata P, Rossi F (1998) Plasticity of the olivocerebellar pathway. *Trends Neurosci* 21:407-413.
- Woo TU, Pucak ML, Kye CH, Matus CV, Lewis DA (1997) Peripubertal refinement of the intrinsic and associational circuitry in monkey prefrontal cortex. *Neuroscience* 80:1149-1158.
- Zhou Q, Homma KJ, Poo MM (2004) Shrinkage of dendritic spines associated with long-term depression of hippocampal synapses. *Neuron* 44:749-757.